INTERNATIONAL JOURNAL OF CLIMATOLOGY
Int. J. Climatol. (2011)
Published online in Wiley Online Library
(wileyonlinelibrary.com) DOI: 10.1002/joc.2429

RMetS
Royal Meteorological Society

Trends in the distributions of aggregated monthly precipitation over the La Plata Basin

Moira E. Doyle,[a,b,c]* Ramiro I. Saurral[a,b,c] and Vicente R. Barros[a,b,c]
[a] *Centro de Investigaciones del Mar y la Atmósfera (CIMA/CONICET-UBA)*
[b] *Departamento de Ciencias de la Atmósfera y los Océanos. Universidad de Buenos Aires*
[c] *UMI IFAECI/CNRS, Buenos Aires, Argentina*

ABSTRACT: Positive trends in annual rainfall in the La Plata Basin (LPB), south of 20 °S observed in the last four decades of the twentieth century were not reversed and became more statistically significant when calculated until 2005. These trends were part of a more general change in the monthly precipitation distribution including extreme precipitation.

Precipitation in dry and extremely dry months (below the 35th percentile) has been decreasing in the whole LPB region south of 22 °S. On the contrary, precipitation in the above normal (between the 65th and 90th percentile) and the extremely high rainfall (above the 90th percentile) ranges has been increasing accounting for most of the annual precipitation trends. More than a steady trend, there has been an abrupt change in extreme monthly precipitation concentrated between 1977 and 1983.

The analysis of intensity and frequency of extreme events was done fitting Generalized Extreme Values (GEV) and Poisson distributions. Each distribution was fitted with and without trends in the location parameter and tested to determine the best fit in each case. The regions where GEV with a positive trend was the best fit coincide with areas affected by extensive floods during the last decades. Spatially aggregated results highlight the signal of change towards higher maximum monthly precipitations for a wide span of return periods.

The atmospheric circulation associated with cases where extreme monthly precipitation was observed in most of the stations was studied through the integrated water vapour transport in the lower troposphere and its associated divergence. During warm months, an intense northern low-level water vapour flow with two convergence nuclei, one over eastern Argentina, southern Brazil and Uruguay, and the other over western Argentina, along with a weakened south Atlantic Convergence Zone was associated with the more extreme precipitation months favouring the occurrence of Mesoscale Convective Systems. Copyright © 2011 Royal Meteorological Society

KEY WORDS trends; GEV; extreme precipitation; water vapour transport; La Plata Basin

Received 11 March 2010; Revised 9 June 2011; Accepted 9 October 2011

1. Introduction

The La Plata Basin (LPB), the fifth largest in the world, extends over five South American countries: Argentina, Bolivia, Brazil, Paraguay and Uruguay (Figure 1). In most of the LPB, large-scale slopes are very small and even in the sub-basins of the Upper Paraná and Uruguay Rivers – where they are bigger – they do not exceed 0.3 m/km (Coronel *et al*., 2006). Hence, when high and extensive rainfall anomalies persist during some months, the combination of broad extensions and small slopes favours river overflows for many months. Lingering floods also take place in the southern part of the basin over the Argentine plains, not only from overflows of rivers and brooks but also from stagnation of the excess water in plains with very small drainage (Latrubesse and Brea, 2009).

Long periods of copious rainfall in LPB leading to extreme discharges were documented by Bischoff *et al.* (2000) for the Uruguay River, Camilloni and Barros (2003) for the Paraná River, and Barros *et al.* (2004) for the Paraguay River. They found, as other authors did (i.e. Berri *et al*., 2002), a strong relationship between extreme discharges and the El Niño phase of ENSO, which is consistent with the association between the El Niño phase and extreme precipitation events in the region (e.g. Grimm *et al*., 2000; Ropelewski and Bell, 2008; Grimm and Tedeschi, 2009). Floods have also been studied in connection with other slow varying climate forcings such as the Atlantic sea surface temperature (Camilloni and Barros, 2004; Muza *et al*., 2009). Although no explicit time scale was formulated in the abovementioned studies, the relationship between floods or extreme discharges and extreme precipitation events was documented at monthly and sometimes seasonal scale.

During the last decades, the media has repeatedly reported flood-related news in the LPB region. In fact, mean river discharges showed a remarkable increase as

* Correspondence to: Moira E. Doyle, Dto. Cs. De la Atmósfera y los Océanos, Ciudad Universitaria. Pabellón II, 2do piso, 1428. Buenos Aires. Argentina. E-mail: doyle@cima.fcen.uba.ar

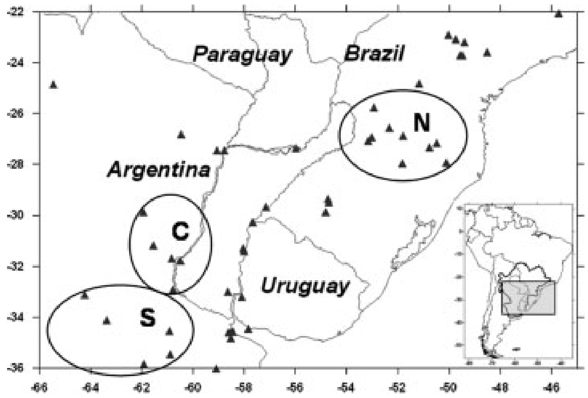

Figure 1. Precipitation stations. In the lower right corner the LPB contour and the area are depicted in the main panel. Circles show the northern (N), central (C) and southern (S) LPB regions.

well as the frequency of extreme discharges did since the 1970s (García and Vargas, 1998; Camilloni and Barros, 2003). This trend can be linked to a similar trend in monthly precipitation extremes. However, until now, the few regional studies dealing with extreme precipitation focused on the daily scale. For instance, Re and Barros (2009) analysed the daily extreme precipitation events over central and northeastern Argentina and over southern Brazil finding positive trends in extreme precipitation frequency events in a region covering most of central Argentina and part of southern Brazil. Penalba and Robledo (2009) also studied extreme daily precipitations over much of Argentina and parts of Uruguay, Paraguay and southern Brazil using percentile analysis, and concluded that there was a trend towards an increase in heavy daily rainfall events (above the 75th percentile) over roughly the same areas found by Re and Barros (2009).

Therefore, one objective of this paper is to analyse the trends in the distribution of the aggregated monthly precipitation over most of LPB (south of 22 °S) during the second part of the twentieth century with special focus on the extreme precipitation months, given their implications on regional floods. North of 22 °S, the scarce data does not allow making trend analyses for that period.

In addition, the paper explores the low-level circulation features predominant in months with extreme precipitation and its relation with Mesoscale Convective Systems (MCS).

These systems are generally associated with heavy precipitation and are frequent in the LPB region accounting for 60–80% of the annual precipitation over a great part of the region (Nesbitt *et al.*, 2006).

2. Data and methodology

Daily precipitation time series were obtained from the National Weather Service of Argentina, the National Meteorological Direction of Uruguay, and the Agência Nacional de Águas (ANA) of Brazil, and were aggregated to obtain monthly totals. Only those stations with less than 0.5% of missing daily data in the January 1960 to December 2005 period (46 years), namely 47 stations, were retained for further elaboration. The station locations are displayed in Figure 1.

Percentiles of monthly precipitation series for each station were calculated using an empirical distribution function with averaging method on the series of precipitation that includes monthly totals of all months. The percentile ranges defined from this distribution do not have the same probability of occurrence throughout the year, since monthly totals of rainiest months will preferably accumulate in the higher percentile ranges, while totals of the driest months will preferably accumulate in the lowest percentile ranges in such distribution. Five different ranges were chosen: below the 10th percentile (extremely dry months), between the 10th and the 35th percentile (dry months), the 35th and the 65th percentile (about normal months), the 65th and the 90th (above normal months), and above the 90th percentile (extremely high rainfall months). Then, for each year, the monthly rainfall amounts falling within each range were added, and the linear trends for each range of each station were calculated applying a linear regression model. The regression coefficients were tested through a t-test (Darlington, 1990). In addition, to assess if the number of months within each range had varied throughout the period analysed, the frequency of months within each range for each year was calculated and a linear trend was fitted to each of these series and tested for statistical significance.

There are two well defined rainfall regimes in the LPB (Grimm *et al.*, 2000). In one case, monthly averaged precipitation has small variations along the year with no distinct dry season. This regime is observed in the N area of Figure 1, and also in Brazil, south of this area, and in northeastern Argentina. In the northern part of the LPB and in western Argentina, instead, the precipitation regime is monsoonal with a pronounced maximum in summer and spring and a minimum in winter and autumn. However, in the boundaries of these two regions, and even inside them, there are important seasonal variations in the annual regime. Hence, it is likely that trends in the distribution of the aggregated monthly precipitation vary with season. Therefore, percentiles for the January–February–March (JFM), April–May–June (AMJ), July–August–September (JAS) and October–November–December (OND) series were calculated and then the total rainfall within each range was added for each season of each year, computing and testing their corresponding linear trends.

The presence of jumps in the annual extreme precipitation series was analysed for each station using the Mann-Whitney-Pettitt test (Pettitt, 1979), which has been used in previous works and shown to be an appropriate tool for this kind of analysis (Kiely, 1999; Franks, 2002). Basically, this method splits time series of length T into two sub-samples ($x_1, \ldots, x_t$ and $x_{t+1}, \ldots, x_T$, in which time t represents the most significant changing point of the time series). The advantage of this method is that it gives a statistical probability for the changing point as well, so the significance of the change can be assessed. A detailed description of the mathematical formulation of the method is given in Kiely (1999).

To relate the occurrence of extremely high monthly precipitation to particular features of the atmospheric circulation, months were ranked, in each season, according to the number of stations exceeding their respective 90th percentile (extremely high rainfall months). The ten months with larger number of stations in the extremely high precipitation range were chosen to compose the water vapour fluxes vertically integrated from 1000 to 700 hPa. The vertically integrated horizontal water vapour flux Q is defined as:

$$Q = \frac{1}{g}\int_{p_t}^{p_s} V \times q \, dp \qquad (1)$$

where V is the mean horizontal wind vector, q is the mean specific humidity, p_t is 700 hPa, and p_s, surface pressure. Then, the anomalies of the monthly water vapour flux and its divergence with respect to their respective trimester long-term mean were calculated. Monthly surface pressure and the horizontal wind and specific humidity fields between 1000 and 700 hPa were obtained from the National Centers for Environmental Prediction-National Center for Atmospheric Research (NCEP-NCAR) 40-Year Reanalysis Project (Kalnay *et al*., 1996).

3. Results

3.1. Background: total precipitation trends

Annual and, in some areas, seasonal positive rainfall trends in southeastern South America during the last decades of the past century were documented in previous studies (i.e. Barros *et al*., 2000, 2008; Haylock *et al*., 2006; Doyle and Barros, 2011). The issue is revisited briefly in this subsection, updating results till 2005, as a background for the percentile trends study.

Linear trends calculated on the annual precipitation series are displayed in Figure 2, highlighting those that are significant at the 5 and 10% confidence levels. All stations show positive trends with values above 5 mm yr^{-1} in almost the whole region east of 60 °W, and a maximum exceeding 8 mm yr^{-1} over northeastern Argentina and southern Brazil. Many of these trends are significant at either the 5 or 10% confidence level, indicating that the upward trend in precipitation over the area is generalized.

In previous studies (Barros *et al*., 2008; Doyle and Barros, 2011), the spatial pattern of trends was similar to the one depicted in Figure 2, though with negative trends in the Upper Paraná Basin, and in some parts of the Pantanal regions that are not analysed here.

In the present analysis, extended until 2005 (Figure 2), the number of stations with significant positive trends is higher than in Barros *et al*. (2008). Thus, trends in rainfall

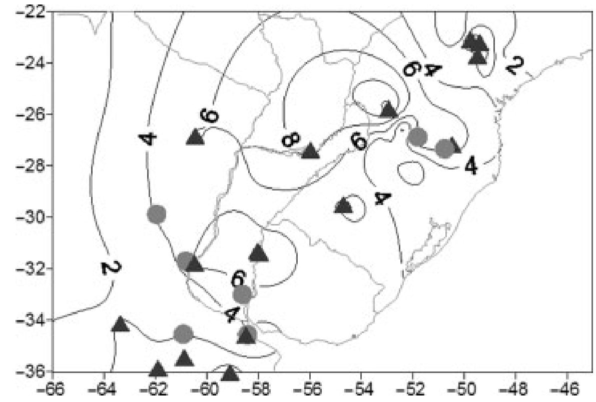

Figure 2. Linear trends of annual precipitation series. Stations where trends are significant at the 5 and 10% levels are shown in black triangles and gray circles, respectively. Values are in mm yr^{-1}.

over the central and southern part of LPB of the last four decades of the last century have become more generalized and were not reversed when calculated including the first five years of the twentyfirst century.

3.2. Percentile trends of the aggregated monthly precipitation

The 10th, 35th, 65th, 90th and 100th percentiles of the monthly precipitation for each station are shown in Figure 3(a–e). For each year, the monthly rainfall amounts falling in each range were added and their linear annual precipitation trends and statistical significance calculated (Figure 3(f–j)).

In the extremely low precipitation range (Figure 3(f)), most of the stations had negative trends (31 out of 47), with a few exceptions located in the northern part of the domain and over central-western Argentina. This pattern is also visible in the dry range (Figure 3(g)), in which almost all the stations had negative trends, and many of them were significant at the 10% and some at the 5% confidence level. The near-climatology range (precipitation falling between the 35th and the 65th percentiles) shows a pattern of positive trends in the east of the domain and negative ones over most of Argentina (Figure 3(h)), while the above-normal (Figure 3(i)) and extremely high rainfall ranges (Figure 3(j)) are characterized by positive trends in almost all stations, many of them statistically significant. The above-90th percentile range trends reach up to 12 mm yr^{-1} over southern Brazil near the border with northern Argentina. Values in Figures 2 and 3 indicate that the above-normal and extremely high monthly precipitation trends over the LPB, south of 22 °S, accounted for most of the total annual precipitation trends during 1960–2005, Though the lower percentile ranges had negative trends, they were smaller and were far from compensating the positive trends of the upper percentiles.

The annual pattern of trends in the upper range percentiles comes primarily from the spring (Figure 4(f–j)) and the autumn (Figure 4(p–t)) trends. In summer and winter, the trends are in general smaller than in the transitional seasons, and their spatial pattern is noisy with even

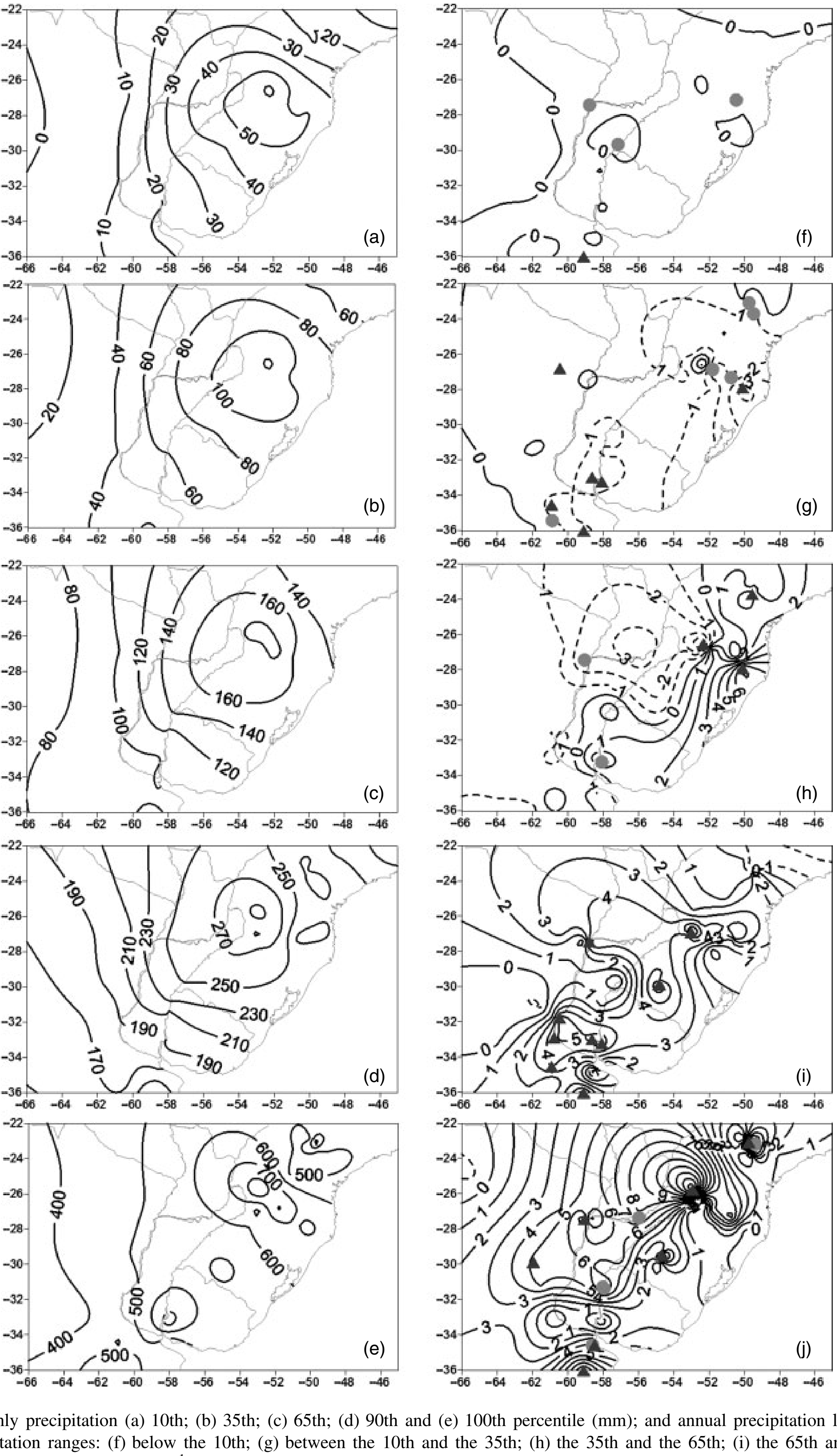

Figure 3. Monthly precipitation (a) 10th; (b) 35th; (c) 65th; (d) 90th and (e) 100th percentile (mm); and annual precipitation linear trends for monthly precipitation ranges: (f) below the 10th; (g) between the 10th and the 35th; (h) the 35th and the 65th; (i) the 65th and the 90th and (j) above the 90th percentile in mm yr^{-1}. Significant trends at the 5 and 10% levels are shown as black triangles and grey circles, respectively. The seasonal dependency in the chosen precipitation in the chosen precipitation percentiles was not taken into account, and therefore, the defined percentile ranges do not have the same probability of occurrence throughout the year (in Section 2).

negative trends in many areas. Also, in the lower percentile ranges, spring and autumn contribute more to the small negative trend than winter and summer; in winter, these ranges have positive trends in most of the region, and in summer, trends are small and spatially noisy.

Trends in monthly precipitation percentile ranges can be caused either by a trend in the frequency of cases within each range or in the average amount of precipitation within the range, or by both. To explore this issue, the changes in the annual frequency of months in each

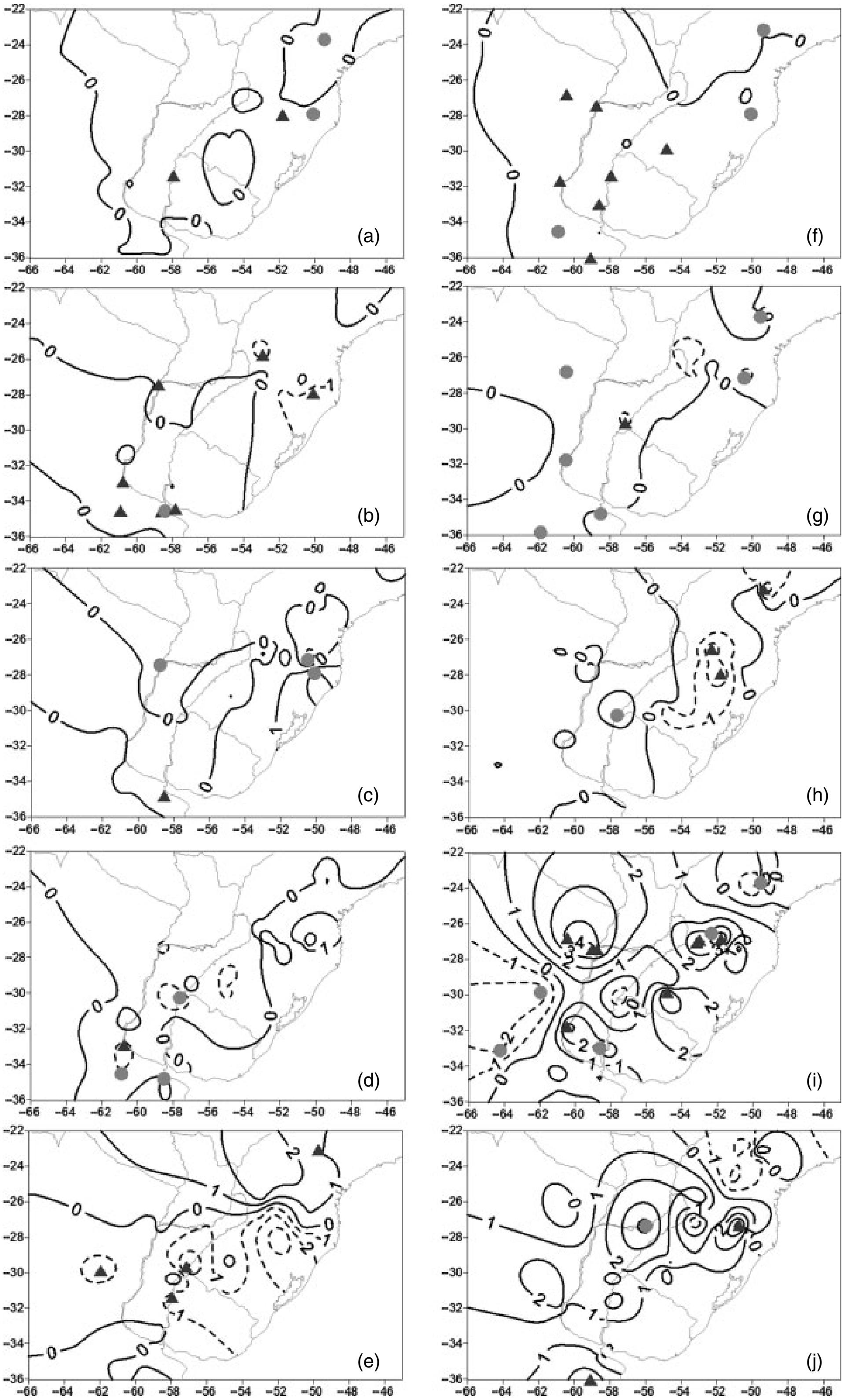

Figure 4. As in Figure 3(f–j), but for winter months (July–September) (a–e) panels, spring months (October–December) (f–j) panels, summer months (January–March) (k–o) panels, and autumn months (April–June) (p–t) panels.

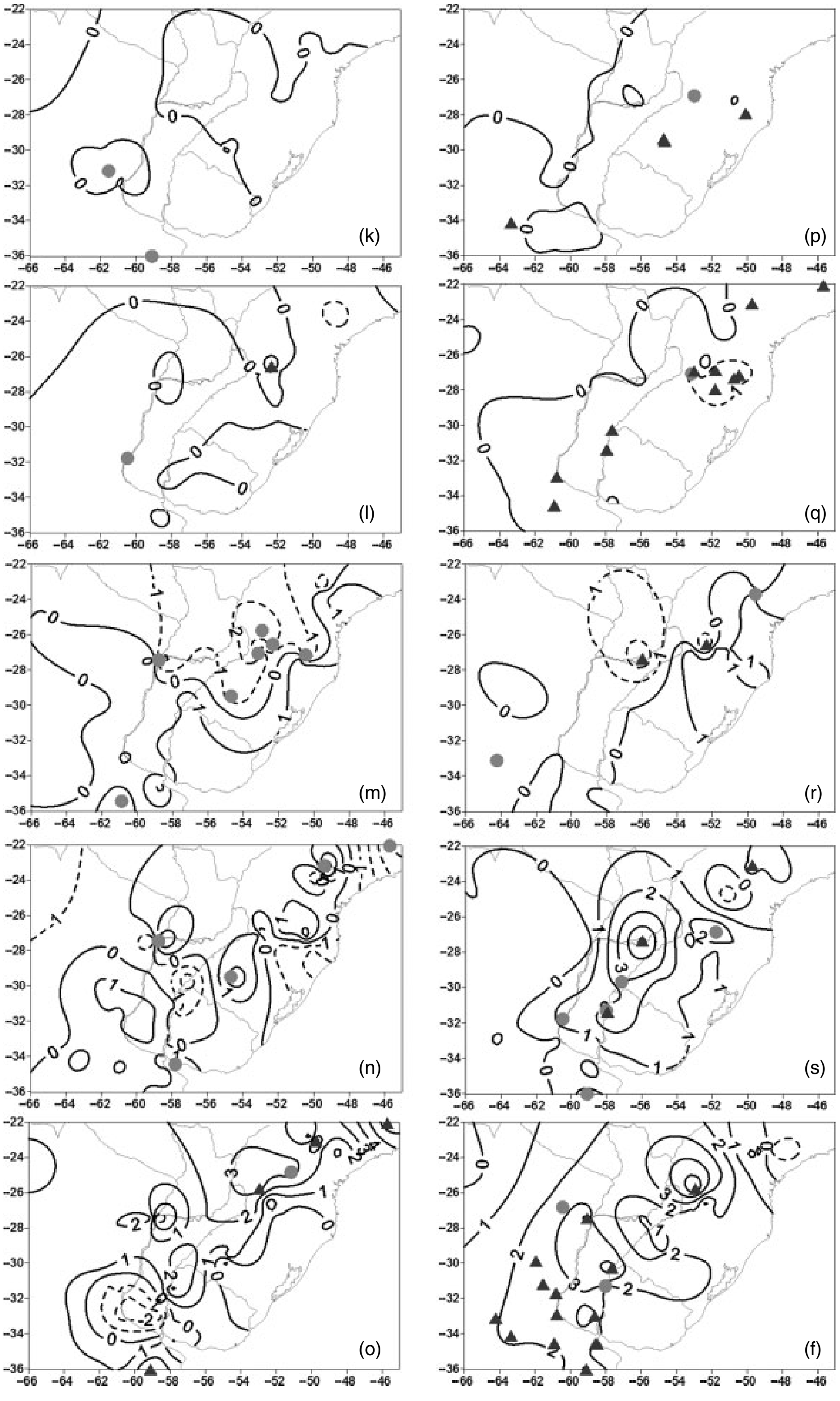

Figure 4. (*Continued*).

precipitation percentile range are shown in Figure 5. It can be seen that, in general, the pattern of these trends is similar to that of the precipitation amounts discussed earlier: the low-precipitation months became less frequent along the period, while months with high precipitation became more frequent. The largest increase in the frequencies of months with extremely high precipitation was in a few stations in the far southern portion of the domain and some in southern Brazil; in both areas, there are stations with upward trends that resulted in an increase of about 1–2 cases in the 46-year period (Figure 5(e)). Since the expected number of cases in the upper 10th percentile for this period is 55, this implies that the increase in the frequency of months with extremely high rainfall should

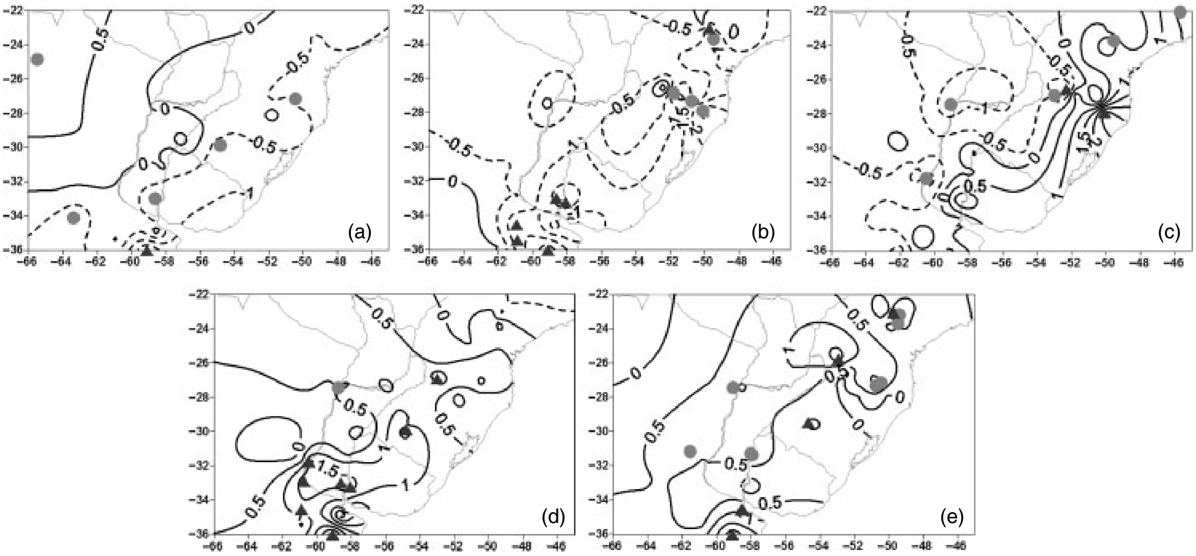

Figure 5. Changes in the annual frequency of months in each range of monthly precipitation resulting from a linear trend in the 46-year period, (a) below the 10th; (b) between the 10th and the 35th; (c) the 35th and the 65th; (d) the 65th and the 90th and (e) above the 90th. Significant changes at the 5 and 10% levels are shown as black triangles and grey circles respectively. The seasonal dependency in the chosen precipitation in the chosen precipitation percentiles was not taken into account, and therefore, the defined percentile ranges do not have the same probability of occurrence throughout the year (in Section 2).

be in the order of 2% and no more than 4%. In the area with an upper limit of about 800 mm in the extreme rainfall range (Figure 3(e)) a 4% increase in the frequency of events explains only less than a 32-mm increase in precipitation for the whole period, against the observed increment of 1 to about 10 mm per year during 46 years (Figure 3(j)). It can be concluded that the increase in rainfall in the upper 10th percentile range of monthly rainfall was basically owing to higher precipitation in this range with only a small contribution from the higher frequency of months with rainfall in this range.

This result does not necessarily imply that heavy daily rainfalls became only more intense and not more frequent. In fact, more frequent heavy two-daily rainfall was reported by Re and Barros (2009) for part of the region, but they can only produce more extreme values in monthly rainfall and not necessarily more frequent extreme rainfall months, indicating no major variations in the seasonality of these rainfalls.

3.3. Jumps or trends in rainfall distributions

Barros *et al*. (2000, 2008) have shown that in the case of northeastern Argentina and eastern Paraguay, rather than a trend, there was a jump in the mean value after 1980, in phase with simultaneous changes in two ENSO indexes, the SST at El Niño 3.4 region and the SOI and although more to the south they found a steady trend in the annual rainfall. Here the possibility of jumps was explored also to the north and south of that region.

Figure 6 shows adjusted Gamma Distributions of monthly rainfall for the spatial average of the three groups of stations corresponding to the regions shown in Figure 1 for three sub-periods: 1960–1975, 1975–1990 and 1990–2005. The mean value reflects a jump from the first to the second period only in region C, consistent with results from Barros *et al*. (2000, 2008). As expected, according to results of section 3.2, in the three regions there was a reduction (increase) of frequencies below (above) the mean value, with a more noteworthy change in the more extreme values in the case of the northern (N) and central (C) stations. These changes in regions N and C took place from the first to the second period with little change afterwards, indicating that an abrupt change, rather than a progressive trend, took place in the monthly precipitation distribution.

An analysis of possible jumps in extreme monthly precipitation was performed to identify the changing points in the series of highest monthly precipitation of each year. The stations with positive changing points in the annual maximum monthly precipitation were 42 while only 4 had a negative changing point in years 1966, 1973, 1976 and 1984. In 16 stations, namely in 1 out of 3, the significance associated with the changing points to a greater maximum monthly precipitation was at 90% level or higher. Most of the positive changing points, 26 out of 42 took place between 1977 and 1983 (Figure 7), indicating that during those years there was an abrupt increase of the maximum monthly precipitation in the majority of the stations. Furthermore, the stations with positive jumps in the maximum monthly precipitation are spread all over the region of the LPB that was analszed here. Therefore, although these jumps took place around the same years as in the case of the annual mean precipitation, their spatial extension was considerably greater.

3.4. Extreme value analysis

To further explore extreme monthly precipitation an extreme value analysis was performed. Monthly extreme precipitation was studied fitting rainfall time series of

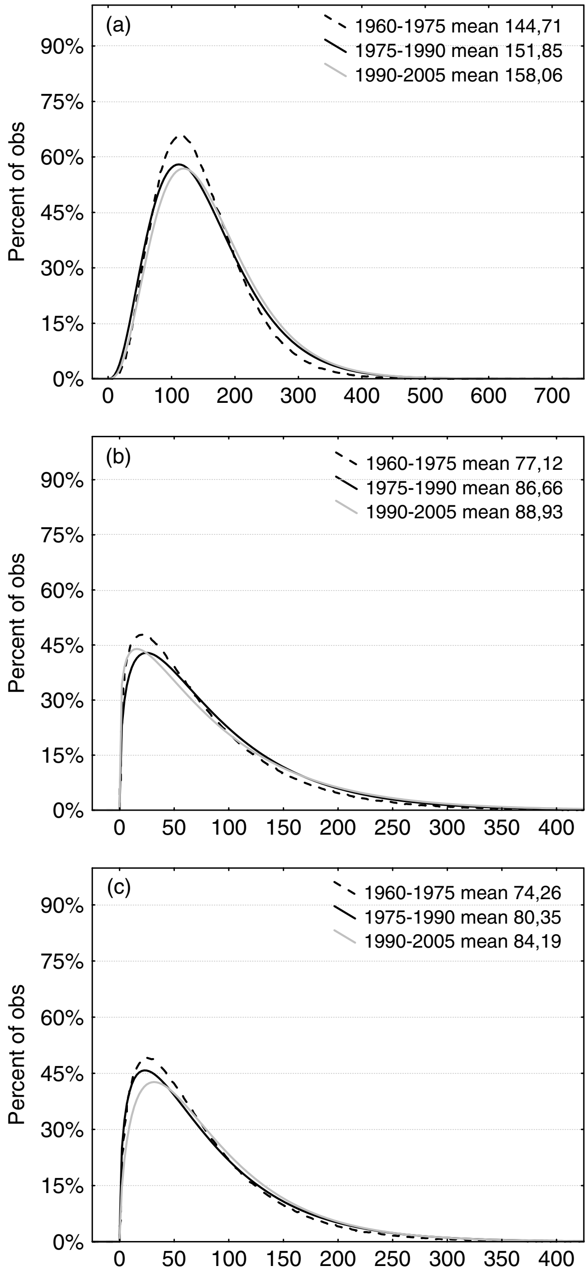

Figure 6. Gamma Distribution of monthly precipitations fitted for periods 1960–1975, 1975–1990 and 1990–2005 averaged for (a) the N; (b) C; and (c) S regions shown in Figure 1. The seasonal dependency in the chosen precipitation in the chosen precipitation percentiles was not taken into account, and therefore the defined percentile ranges do not have the same probability of occurrence throughout the year (in Section 2).

each station to the Generalized Extreme Values distribution (GEV;Coles, 2001),

$$G(z) = \exp\left[-\left(1 + \gamma \cdot \frac{z-\mu}{\sigma}\right)^{-\frac{1}{\gamma}}\right] \qquad (2)$$

where μ is the location parameter (conceptually similar to the mean in a normal distribution), σ is the scale parameter (similar to the standard deviation), and γ is the shape parameter, which determines the tail behavior of the distribution. To fit the GEV distribution, data was grouped into blocks of the same length and the largest value in each sub-sample was considered for the analysis (Block Maxima Approach (BMA)). In this case, the month with the highest rainfall amount of each year was considered, leading to a series of 46 values for each location. GEV distributions were fitted, with and without linear trends in the location parameter and then tested through a likelihood-ratio test (Nadarajah, 2005) to determine whether or not the fit with the trend was significantly better than the one with no trend (Coles, 2001).

Results of the GEV analysis are shown in Figure 8. None of the stations fits to a GEV distribution with a negative trend in the location parameter. Although the majority of the stations fit better to the GEV distribution without trend in the location parameter, in more than a third of the series, 17 out of 47 – mainly over central Argentina, and also over southern Brazil – the model with the linear trend is significantly better. It is worth noting that the stations in central Argentina where there was a positive linear trend in the GEV location parameter are located in areas that have suffered from extensive plain or river-related floods during the last part of the twentieth century and also early this century (Latrubesse and Brea, 2009). It is also the case of the stations in the Upper Paraná Basin between 23 °S and 28 °S, an area where most of the streamflows that led to floods downstream originated during the last decades (Camilloni and Barros, 2003).

The stations with best fit of the GEV to a linear trend in the location parameter (triangles in Figure 8) are also stations with significant trends in the annual precipitation. In Argentina, seven of nine stations with a GEV best fitting with a linear trend coincide with stations with significant trends in annual precipitation, while in Brazil the coincidence is six out of eight. This is consistent with the fact that most of the annual precipitation trends are explained by the monthly precipitations of the upper percentile ranges as shown before.

The fact that 64% of stations did not adjust best to a GEV distribution with a positive trend included can be explained by a lack of significance in the otherwise vigorous trends in the extremely high precipitation range (Figure 3(j)). The poor statistical significance of extreme monthly precipitation may be due to the high variability of the heavy convective precipitations, which in southeastern South America is the major fraction of annual precipitation (Nesbitt *et al*., 2006).

Since the monthly precipitation maximum of every year showed a generalized jump in the 1977–1983 period, its implications on the maximum monthly precipitation corresponding to a wide range of return periods were explored. The GEV distribution was adjusted for each station to monthly maximums for three different periods: before the time of the generalized jump, namely 1960–1975 and for two subsequent periods, 1976–1990 and 1990–2005.

The percentage of stations showing an increase in the maximum monthly precipitation expected for a given

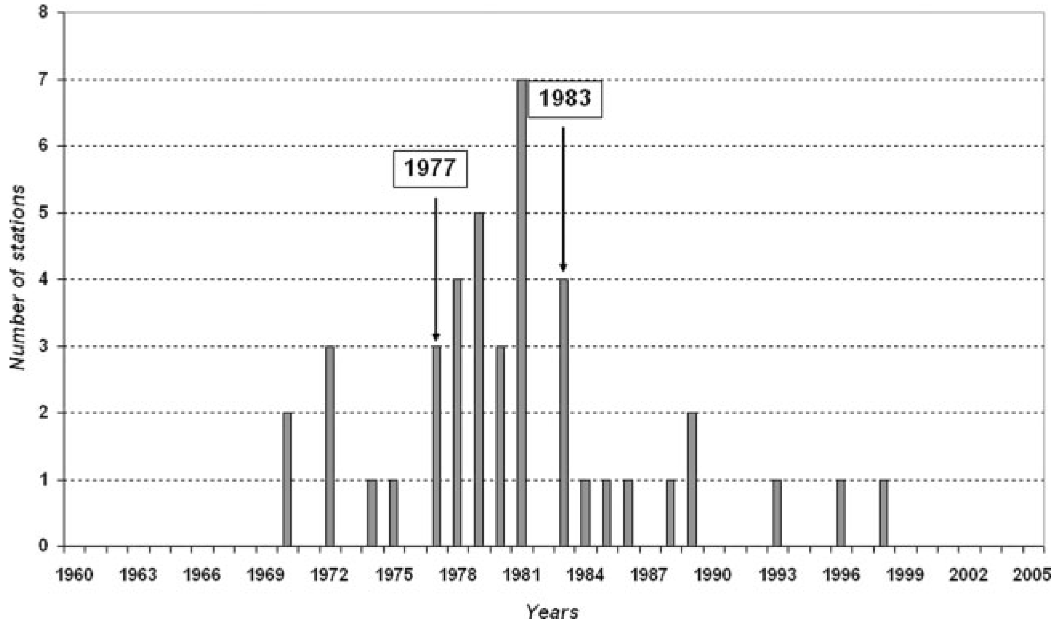

Figure 7. Number of stations with their changing points falling in the different years. The years 1977 and 1983 are highlighted as they are around the start and end of the periods in which most stations had their changing points.

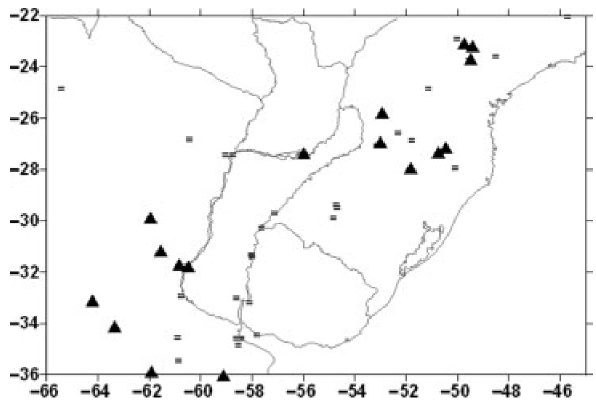

Figure 8. GEV distribution fit to each precipitation series. Triangles indicate stations which fit best to a GEV distribution with a positive trend in the location parameter, and the equal signs indicate stations adjusting best to a no-trend approach.

Table I. Percentage of stations with an increase in the amount of the precipitation level for the return periods as shown.

Return period (years)	1990–2005 with respect to 1960–1975%	1990–2005 with respect to 1975–1990%
2	77	64
3	81	60
5	81	57
10	81	53
15	81	53
20	77	53
25	72	53
30	74	51
50	70	49
60	70	49
70	66	49
100	64	49
150	66	51

return period is shown in Table I. It can be seen that, in most stations, there was a positive jump in this maximum precipitation from the first to the second period, roughly in 80% of the stations for return periods from 2 to 20 years and about 65–70% for longer return periods. On the other hand, the number of stations with increased maximum monthly precipitation from the second to the third period is lower for all return periods and about 50%, the expected frequency in the case of no change, for return periods of 10 years or more.

The jump from the first to the second period is more visible when the maximum level corresponding to each return period is averaged over all stations (Figure 9). The average of the maximum monthly precipitation values during the first period (1960–1975) were smaller for all return periods than in the two other periods, while the differences between the second and third periods are very small. Considering only the 1960–1975 period, the once-in-a-century monthly extreme precipitation was about 460 mm, while using data from any of the two other periods leads to a value of nearly 620 mm. The close proximity of the 1975–1990 and 1990–2005 curves confirms the jump in the maximum annual values observed at the beginning of the 1975–1990 period.

Figure 10 shows the range of differences in the maximum monthly precipitation computed for selected return periods and for all stations, using GEV parameters derived for the periods 1960–1975 and 1975–2005. It can be seen that the median over the stations is always positive and, although there is a large spread among the

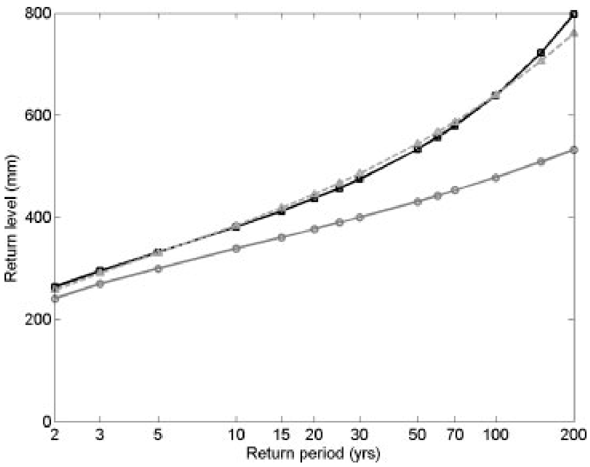

Figure 9. Return levels (in mm $month^{-1}$) for different return periods (in years) as derived from GEV fits in periods 1960–1975 (solid gray line with circles), 1975–1990 (dashed gray line with triangles), and 1990–2005 (solid black line with squares).

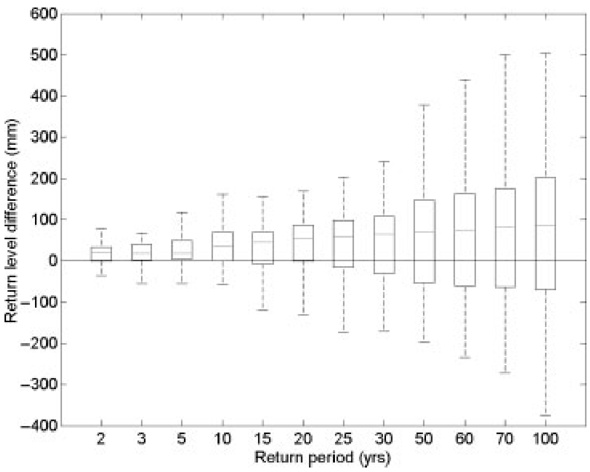

Figure 10. Box plot of the difference in return levels derived from GEV data for the period 1975–2005 minus 1960–1975 for the 47 stations used in this study. Boxes have lines at the lower quartile, median and upper quartile values, and the outside whiskers show the extent of the data (i.e. the extreme changes among all the stations considered in the analysis).

different stations, particularly for large return levels, there are more stations with an increase in the return level for all return periods. The higher frequency of extreme events does not explain the higher total precipitation, as already discussed, but it has, however, an important practical importance for engineering and water resource management. In fact, overlooking the presence of this important change in extreme precipitations has led, in some cases, to erroneous decisions in the water management (Cámara Argentina de la Construcción, 2003).

To analyse the frequency of extreme events, a Poisson Distribution (PD) was fitted to the annual frequency of monthly precipitation over a threshold. Its distribution function can be written as

$$F(x) = \frac{e^{\lambda} \cdot \lambda^{x}}{x!} \quad (3)$$

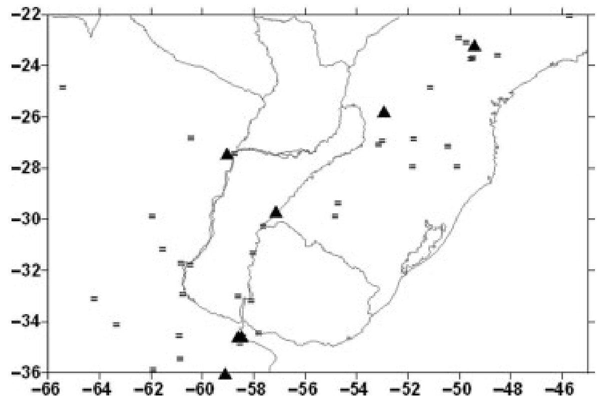

Figure 11. As in Figure 8, but for the Poisson distribution and with a positive trend applied to the λ parameter.

with λ being at the same time the mean and variance of this distribution.

PD analysis was similar to that of GEV, although in this case the analysis was for exploring trends in the frequency of occurrence of extreme precipitation. The 90th percentile was chosen as the threshold above which events were considered for the PD analysis. Figure 11 displays the stations to which PD fits best with and without a linear trend in the λ parameter. None of the stations fits well to a PD with a negative trend, but very few stations display significant positive trends in the frequencies of extremes, while the rest show no trend in the frequency. This indicates once again that, over most of the region, the positive trends of the annual totals corresponding to monthly rainfalls in the extremely high rainfall range are mainly because of increasing monthly precipitation within this range rather than to a raise in the frequency of these extremely rainy months.

3.5. Atmospheric circulation anomalies related to extreme monthly precipitations

The number of stations in the region that exceeded its 90th percentile varied from 31 of the 47 stations in the rainiest region-wide month (December 1965) to 22 of the 47 stations in the 10th rainiest month (April 1986). Of these ten months, four were in November–December, three in January and four in April–May. It is worth mentioning that, although in most of the stations used in this study January is not the rainiest month, it was, however, the month with more cases in the top ten with more stations over the 90th percentile. When the 20 top months are ranked with the same criterion, there are cases in all calendar months, except August These results indicate that while the more extended events over the region of extreme monthly precipitations may occur at any time in the year, there is however a bias towards the warmer months.

Monthly precipitation extremes generally result from several precipitation events that are likely embedded in a circulation that favours warm and humid advection (moisture influx from the tropical continent) and dynamic lift over the region. Hence, the composite of the 1000–700 hPa integrated moisture flux anomaly and

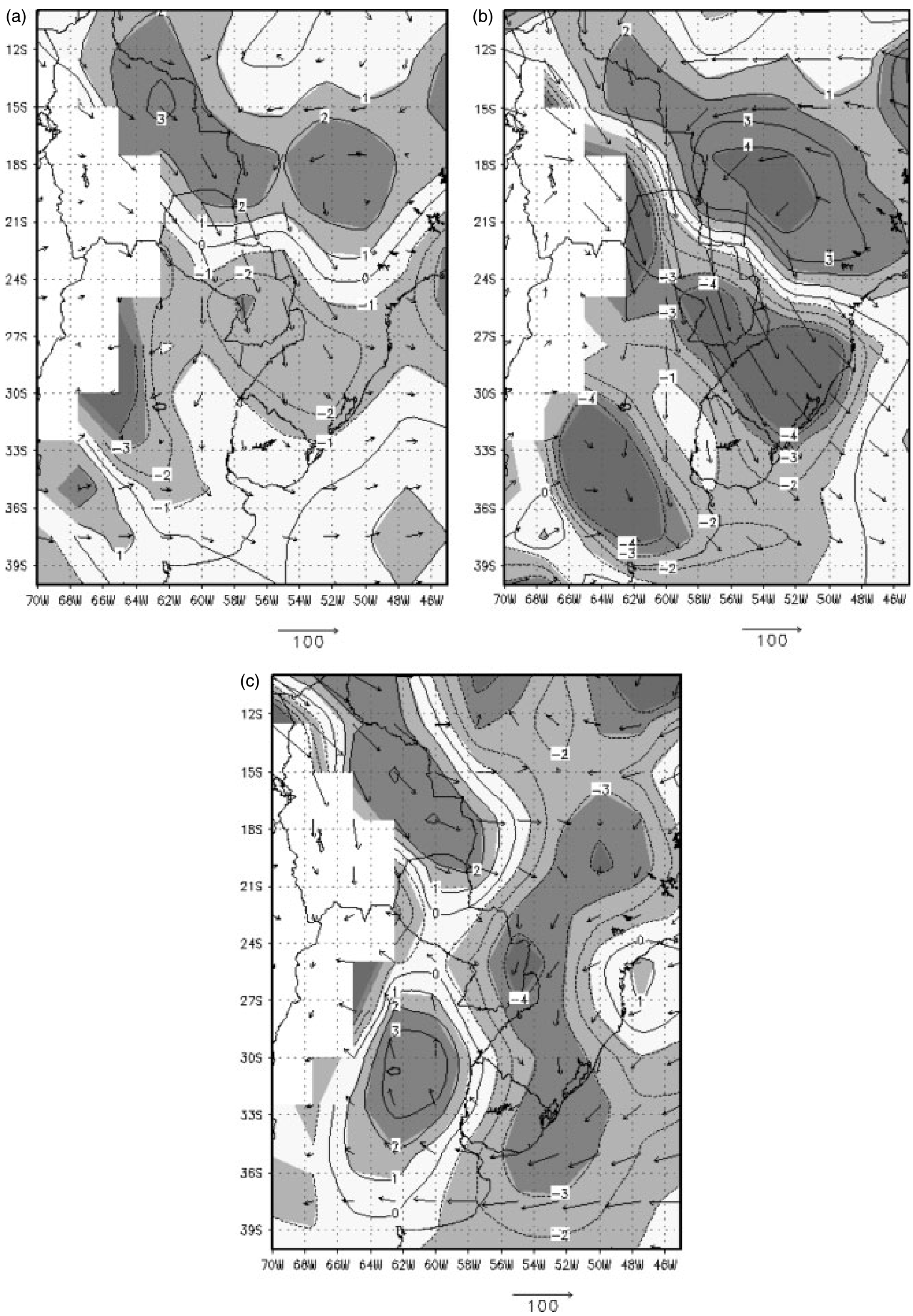

Figure 12. 1000–700 hPa vertically integrated water vapour flux composite anomaly, of the composite of the months with most stations exceeding their corresponding 90th percentile (vectors, mm m s^{-1}), and associated horizontal divergence (shaded, in 10^{-5} mm s^{-1}). Regions with topography above 1500 m are blanked out, (a) December 1965 and 1991 and November 1982 and 1986, (b) January 1970, 1990 and 2001, and (c) April 1986 and 1998, and May 1983.

its associated divergence field for the 10 months in which the largest number of stations in the region exceeded the 90th percentile were calculated and composed in three groups, November–December, January and April–May (Figure 12).

It can be seen that during these warm months (November, December and January) (Figure 12(a–b)), there is an enhancement of the horizontal moisture convergence over most of the subtropical continent, east of the Andes and south of 25 °S. There are two nuclei of convergence: one in the eastern part of LPB, where most of the stations that are used in this study are located, and the other along western and central Argentina. The first nucleus of convergence is in the path of an enhanced low-level water vapour flux from the northwest, very much as in the cases in which the South Atlantic Convergence Zone (SACZ) is in its weak phase (Nogués-Paegle and Mo, 1997). In fact, over Brazil, in the region where in the case of the strong phase of the SACZ an eastward low-level flow coming from the Amazon prevails, there are dominant westward anomalous flows and anomalous divergence; these features extend also into the SACZ region itself (Figure 12). These features are a relevant part of the regional intraseasonal variability, but are also seen at the interannual time scale (Doyle and Barros, 2002; Grimm and Zilli, 2009).

Another feature of the extremely rainy-month composite of these months, which is not always in the weak phase of the SACZ, is a second nucleus of convergence over northwestern and central Argentina in the path of the western part of the low-level moisture flux that has a southward direction along central Argentina. In this western region, very few stations enter into this study, and therefore, the convergence in the composite field results from an indirect connection with extreme rainfall months in the eastern nucleus. This feature is consistent with the first and second modes of the interannual variability of summer precipitation found by Grimm and Zilli (2009; in their Figs. 3a, c) and also with the wind field correlation with the first summer mode of precipitation (their Figure 8b).

One possible explanation of the connection between the low-level convergence of moisture in western Argentina with the composite of more rainy months in southeastern South America is that extreme rainfall months in this region result from the occurrence of MCS that generally originate in western and central Argentina in the eastern slopes of the mountains that run parallel to the Andes, west of 65 °W, and then move eastwards (Salio *et al*., 2007) accounting for about 60% of the annual precipitation of the region (Nesbitt *et al*., 2006). The occurrence of MCS is highly correlated with the events of the Low Level Jet (LLJ), which sometimes is embedded in the northern flow branch during the weak phase of the SACZ (Nicolini *et al*., 2002). More specifically, Salio *et al*. (2007) found that the MCS developing over central and northern Argentina associated with LLJ events were accompanied by two areas of maximum moisture flux convergence: one over northeastern Argentina and southern Brazil, and a secondary one centred over western Argentina at about 65 °W (their Fig. 8). This suggests that these individual events also have a signature in the monthly mean field, given that the convergence pattern shown in Figure 12 is very similar to that MCS-related field.

The frequency of MCS during months with greater number of stations over the 90th precipitation percentile was estimated from the GOES satellite imagery database of NOAA (available at http://www.ncdc.noaa.gov/gibbs/) identifying the region of their origin, whether they originated east or west of 60 °W (which is roughly the meridian that separates the two convergence nuclei; Figure 12). Since December 1965 and January 1971 could not be considered in this analysis because geostationary imagery was not yet available in those periods, only five months of the top ten remained for this analysis. Therefore, to gain more representativeness, the three following cases were added: namely February 1984, December 1997 and March 2002. A total of 72 MCSs were identified, with an average of 9 MCS per month, which is a high rate of almost one every three days. Of the 72 MCS, 52 developed west of 60 °W and then moved eastward, towards the region east of 60 °W, while 19 systems originated and reached their maximum intensity east of 60 °W. Only one MCS formed and dissipated west of 60 °W. Thus, there was a predominant pattern in which MCS developed over the mountain region of central and northwestern Argentina and then moved eastwards, as also suggested by the moisture flux anomalies convergence fields for the warm semester (Figure 12(a–b)).

As a conclusion, it can be said that during the warm part of the year, extremely rainy months over eastern Argentina, Uruguay and southern Brazil occur when the SACZ is weaker and there is a convergence of low-level moisture flux, not only over the east of LPB, but over northwest and central Argentina that favours the formation of MCS.

During cold season, the SACZ is inactive, and the higher precipitation over the region tends to develop over Uruguay and southern Brazil, related to the passage of cyclonic perturbations and cold fronts (Vera *et al*., 2002). During the extremely rainy months of April–May there was an enhanced low-level moisture coming from the Amazon, crossing northern Bolivia, Paraguay and ending in a convergence nucleus in Brazil at 20 °S, 50 °W, but also continuing over the eastern part of the region along the Brazilian coast; however, most of this flow in this region comes from the Atlantic (Figure 12(c)). These two branches produce a convergence region over northeastern Argentina, southern Brazil and Uruguay. As in the warm months, there is also a second region of convergence of the low-level water vapour flux anomaly, but only in northwestern Argentina that has probably the same connection to the extreme rainfall in the east side of LPB as in the warm part of the year, namely the starting up of the MCS. In fact, these systems are frequent in April and May (Salio *et al*., 2007) although, of course, they are more constrained towards lower latitudes than in the warmer months.

It was still not possible to assess if the trend in the extreme monthly precipitation was because of more intense or frequent MCS, or because of other factors. Satellite information suitable for MCS analysis was not available before the time of the abrupt increase of the extremely high precipitation, and other meteorological information was not dense enough in time and space.

4. Conclusions

The positive trends in rainfall over the central and southern part of LPB observed during the last four decades of last century (Barros *et al.*, 2008) were not reversed during the first five years of the twentyfirst century and, on the contrary, in the 1960–2005 period, more stations distributed all over the region showed statistically significant positive trends.

These positive trends of the annual precipitation over the La Plata Basin, south of 22 °S, was part of a change that modified the aggregated monthly precipitation distributions, including positive changes in its upper extreme ranges in most of the stations (Figure 3). There was a negative trend in the amount of precipitation and in the frequency of dry and extremely dry months (i.e. those below the 35th percentile) while, on the other hand, there was a positive and, in many cases, significant trend in the above normal monthly precipitation (over the 65th percentile). The above-normal, and especially the over-90th percentile range trends accounted for most of the annual precipitation trends over large areas (Figures 2 and 3). The trends in these percentile ranges come primarily from the spring and especially from the autumn with little or no contribution from winter and summer (Figure 4).

Although the atmospheric mechanisms related to precipitation vary along the year (Rao and Hada, 1990; Gan and Rao, 1991; Vera *et al.*, 2002; Nesbitt *et al.*, 2006), the more extreme monthly precipitations events, which extends over a great part of the region may occur at any time of the year. However, there is a clear bias towards the warmer months. Consequently, the fact that trends in the upper ranges of the precipitation distribution of monthly rains took place in the intermediate seasons may indicate that certain atmospheric features which are more frequent in the warmer months and are associated to the upper range precipitation events, were expanded to the intermediate seasons.

Changes in the monthly precipitation distributions were in many cases not steady but rather abrupt and concentrated around the 1970 and 1980 decades as suggested by the Gamma Distribution analysis in three sub-regions in the north, centre and south of the area of this study (Figure 6). This abrupt change was also observed in the annual maximum monthly precipitation. Most of the records, namely 90%, corresponding to stations spread all over the LPB region, had positive changing points, with significance at 90% level in almost 40% of them. The positive changing points were concentrated in a few years between 1977 and 1983 when they took place in 55% of the stations (Figure 7). The analysis of the annual monthly maximum precipitation with the GEV distribution was less conclusive; although no series fitted best to a negative trend, only one third of them did it to a positive trend better than to a non-trend distribution. Since extreme precipitations are highly variable, even at monthly scale, especially when they are based on measurements at a single rain gauge, other approaches considering averages over the region or sub-regions can produce a clearer signal. Thus, a jump from the 1960–1975 years, and the subsequent similar length periods, was observed in the maximum monthly precipitation level for a span of return periods from 2 to 150 years, which was calculated from the GEV distribution for each station and then averaged over all stations (Table I).

These results indicate that monthly extreme precipitations were more important since the late 1970s. Given that most of the basin has a slow runoff because of its prevailing small land slopes, this change in the extreme monthly precipitations was reflected in more frequent long-lasting extreme floods (Camilloni and Barros, 2003; Barros *et al.*, 2004; Latrubesse and Brea, 2009). Therefore, the changes in the precipitation distribution, and especially in the more extreme precipitations, had important implications for water management practices; floods in Argentina alone caused the evacuation of hundreds of thousands of people and estimated costs of over a billion dollars on several occasions during the last decades (Nuñez and Vargas, 1998; Latrubesse and Brea, 2009).

The low-level atmospheric circulation associated with the occurrence of extremely wet months over most of LPB south of 22 °S was characterized by positive anomalies of the low-level water vapour flux into the region as well as of its convergence (Figure 12(a–b)). In the warm months, this convergence occurred over northern Argentina and also over western Argentina with anomalous divergence over the SACZ region. Thus, in the warm months, the more extremely rainy months stretching over LPB south of 22 °S occurred when the SACZ is less active and there was enhanced low-level water vapour flow and convergence not only over the LPB region itself, but also over western Argentina. The last condition results from the fact that the majority of the MCS that account for a great part of warm-season precipitation in most of LPB are initiated in western Argentina. In the case of the autumn, the positive anomaly of low-level water vapour convergence was located more to the east over Uruguay and southern Brazil, but again was accompanied by a second nucleus, this time more to the north, over northwestern Argentina (Figure 12(c)). This relationship between the low-level atmospheric circulation, the MCS and the most extreme monthly precipitations could be used to explore the causes of the abrupt increase of these precipitations, going back in time before the period with satellite information, suitable for MCS analysis.

Acknowledgments

The research leading to these results has received funding from the European Community's Seventh Framework Programme (FP7/2007-2013) under Grant Agreement N° 212492, and from ANPCYT Grant PICT2007-00400.

References

Barros VR, Castañeda ME, Doyle ME. 2000. Recent precipitation trends in Southern South America East of the Andes: an indication of climatic variability. *Southern Hemisphere paleo- and neoclimates.*

Key sites, methods, data and models, Smolka PP, Volkheimer V (eds). Springer: Berlin, 187–206.

Barros VR, Chamorro L, Coronel G, Báez J. 2004. The major discharge events in the Paraguay River: magnitudes, source regions and climate forcings. *Journal of Hydrometeorology* **5**: 1161–1170.

Barros VR, Doyle ME, Camilloni I. 2008. Precipitation trends in southeastern South America: relationship with ENSO phases and the low-level circulation. *Theoretical and Applied Climatology* **93**: 19–33.

Berri GJ, Ghietto MA, García NO. 2002. The influence of ENSO in the flows of the Upper Paraná River of South America over the past 100 years. *Journal of Hydrometeorology* **3**: 57–65.

Bischoff S, García N, Vargas W, Jones P, Conway D. 2000. Climatic variability and Uruguay River flows. *Water International* **25**: 446–456.

Cámara Argentina de la Construcción. 2003. El cambio climático y sus consecuencias territoriales. (Climate change and its field consequences) 51st Annual Meeting. Buenos Aires.

Camilloni I, Barros V. 2003. Extreme discharge events in the Paraná River and their climate forcing. *Journal of Hydrology* **278**: 94–106.

Camilloni I, Barros V. 2004. La temperatura del Atlántico Sur y la diferencia de caudales del Río Paraná durante los eventos El Niño 1982-83 y 1997-98. *Revista Brasileira de Meteorología* **19**: 35–47.

Coles S. 2001. *An introduction to statistical modeling of extreme values*. Springer: London.

Coronel G, Menéndez A, Chamorro L. 2006. Fisiografía e hidrología de la Cuenca del Plata. *El Cambio Climático en la Cuenca del Plata*, Barros V, Clarke R, Silva Dias P (eds). CIMA-CONICET: Buenos Aires 81–92.

Darlington RB. 1990. *Regression and linear models*. McGraw-Hill: New York.

Doyle ME, Barros VR. 2002. Midsummer low-level circulation and precipitation in subtropical South America and related sea surface temperature anomalies in the South Atlantic, 2002. *Journal of Climate* **15**: 3394–3410.

Doyle ME, Barros VR. 2011. Attribution of the river flow growth in the Plata Basin. *International Journal of Climatology.* DOI: 10.1002/joc.2228.

Franks SW. 2002. Identification of a change in climate state using regional flood data. *Hydrology and Earth System Sciences* **6**: 11–16.

Gan MA, Rao VB. 1991. Surface cyclogenesis over South America. *Monthly Weather Review* **119**: 1293–1302.

García N, Vargas W. 1998. The temporal climate variability in the Rio de la Plata basin displayed by river discharges. *Climate Change* **38**: 359–379.

Grimm AM, Barros V, Doyle M. 2000. Climate variability in southern South America associated with El Niño and La Niña events. *Journal of Climate* **13**: 35–58.

Grimm AM, Tedeschi RG. 2009. ENSO and extreme rainfall events in South America. *Journal of Climate* **22**: 1589–1609.

Grimm AM, Zilli MT. 2009. Interannual variability and seasonal evolution of summer monsoon rainfall in South America. *Journal of Climate* **22**: 2257–2275.

Haylock MR, Peterson TC, Alves LM, Ambrizzi T, Anunciação YMT, Baez J, Barros VR, Berlato MA, Bidegain M, Coronel G, Corradi V, Garcia VJ, Grimm AM, Karoly D, Marengo JA, Marino MB, Moncunill DF, Nechet D, Quintana J, Rebello E, Rusticucci M, Santos JL, Trebejo I, Vincent LA. 2006. Trends in Total and Extreme South American Rainfall in 1960–2000 and Links with Sea Surface Temperature. *Journal of Climate* **19**: 1490–1512.

Kalnay E, Kanamitsu M, Kistler R, Collins W, Deaven D, Gandin L, Iredell M, Sha S, White G, Woollen J, Zhu Y, Chelliah M, Ebisuzaki W, Higgins W, Janowiak J, Mo KC, Ropelewski C, Wang J, Leetmaa A, Reynolds R, Jenne R, Joseph D. 1996. The NCEP/NCAR 40-year Reanalysis Project. *Bulletin of the American Meteorological Society* **77**: 437–471.

Kiely G. 1999. Climate change in Ireland from precipitation and streamflow observations. *Advances in Water Resources* **23**: 141–151.

Latrubesse EM, Brea D. 2009. Floods in Argentina. *Developments in Earth Surface Processes* **13**: 333–349.

Muza M, Carvalho LMV, Jones C, Liebmann B. 2009. Intraseasonal and interannual variability of extreme dry and wet events over southeastern South America and the subtropical Atlantic during austral summer. *Journal of Climate* **22**: 1682–1699.

Nadarajah S. 2005. Extremes of daily rainfall in West Central Florida. *Climatic Change* **69**: 325–342.

Nesbitt SW, Cifelli R, Rutledge SA. 2006. Storm morphology and rainfall characteristics of TRMM precipitation features. *Monthly Weather Review* **134**: 2702–2721.

Nicolini M, Saulo AC, Torres JC, Salio P. 2002. Enhanced precipitation over southeastern SouthAmerica related to strong low-level jet events during austral warm season. *Meteorológica* **27**: 89–98.

Nogués-Paegle J, Mo KC. 1997. Alternating wet and dry conditions over South America during summer. *Monthly Weather Review* **125**: 279–291.

Nuñez MN, Vargas WM. 1998. El Niño 1997/98: un factor económico y social. *Boletin Informativo Techint*. **295**: 9–36.

Penalba OC, Robledo FA. 2009. Spatial and temporal variability of the frequency of extreme daily rainfall regime in the La Plata Basin during the 20th century. *Climatic Change* **98**: 531–550.

Pettitt AN. 1979. A nonparametric approach to the change point problem. *Journal of the Royal Statistical Society. Series C (Applied Statistics)* **28**: 126–135.

Rao VB, Hada K. 1990. Characteristics of rainfall over Brazil: Annual variations and connections with the Southern Oscillation. *Theoretical and Applied Climatology* **42**: 81–91.

Re M, Barros VR. 2009. Extreme rainfalls in SE South America. *Climatic Change* **96**: 119–136.

Ropelewski C, Bell M. 2008. Shifts in the statistics of daily rainfall in South America conditional on ENSO phase. *Journal of Climate* **21**: 849–865.

Salio PV, Nicolini M, Zipser EJ. 2007. Mesoscale convective systems over southeastern South America and their relationship with the South American Low-Level Jet. *Monthly Weather Review* **135**: 1290–1309.

Vera C, Vigliarolo P, Berbery E. 2002. Cold season synoptic-scale waves over subtropical South America. *Monthly Weather Review* **130**: 684–699.

